Journal of Applied Mathematics and Physics, 2025, 13(8), 2593-2607
https://www.scirp.org/journal/jamp
ISSN Online: 2327-4379
ISSN Print: 2327-4352

# Entropy Generation in an Unsteady Reactive Viscous Flow in a Porous Cylindrical Pipe with an Isothermal Wall

**Philip Iyiola Farayola[1], Lateefat Olanike Aselebe[2], Tajudeen Motunrayo Asiru[1*], Kafilat Adebimpe Salaudeen[1], Saheed Dolapo Ogundiran[3]**

[1]Department of Mathematics, Emmanuel Alayande University of Education, Oyo, Nigeria
[2]Directorate of General Studies (Mathematics Unit), Federal School of Surveying, Oyo, Nigeria
[3]Department of Pure and Applied Mathematics, Ladoke Akintola University of Technology, Ogbomoso, Nigeria
Email: farayola_pi@yahoo.com, loaselebe@fss-oyo.edu.ng, *tunra2014@yahoo.com, salaudeenka@gmail.com, ogundiransaheed81@gmail.com

**How to cite this paper:** Farayola, P.I., Aselebe, L.O., Asiru, T.M., Salaudeen, K.A. and Ogundiran, S.D. (2025) Entropy Generation in an Unsteady Reactive Viscous Flow in a Porous Cylindrical Pipe with an Isothermal Wall. *Journal of Applied Mathematics and Physics*, **13**, 2593-2607.
https://doi.org/10.4236/jamp.2025.138147

**Received:** May 25, 2025
**Accepted:** August 17, 2025
**Published:** August 20, 2025



## Abstract

Heat and mass transfer in porous media have critical applications in engineering, groundwater management, and oil recovery. Reactive flows, involving chemical reactions within the fluid phase, generate heat, presenting challenges in thermal systems. This study gives the theoretical and practical analysis of entropy generation in the unsteady flow of a reactive viscous fluid through a porous circular pipe under Arrhenius kinetics. The flow is modeled as an unsteady incompressible viscous fluid subjected to a pressure gradient, with constant wall temperature. Key parameters such as permeability, Prandtl number, and viscous heating are analyzed for their impact on entropy generation. Results indicate that the entropy generation peaks near the pipe wall, with maximum values observed between r = 0.8 and r = 0.9 from the centre. Entropy increases with high permeability until a critical value of 4.2887, beyond which it diverges. Similarly, increases in the Prandtl number and viscous heating parameter enhance entropy generation, particularly midway toward the wall. These findings provide insights into minimizing entropy in reactive flow systems.

## Keywords

Entropy Generation, Reactive Viscous Flow, Porous Pipe, Unsteady Flow, Thermodynamics, Isothermal Wall

## 1. Introduction

Entropy is a fundamental thermodynamic concept that quantifies the degree of

disorder within a system and is pivotal for understanding process irreversibility [1]. According to the second law of thermodynamics, systems naturally progress towards higher entropy unless external energy is applied to maintain order [2]. In reactive flow systems, factors such as heat transfer, mass diffusion, and chemical reactions contribute to entropy production, which impacts energy efficiency by increasing energy loss and degrading system performance. The principles of thermodynamics, particularly the first and second laws, form the basis for analyzing thermofluid systems. Entropy production, indicative of irreversibility in complex processes, is crucial for optimizing industrial designs including solar energy collectors, electronic cooling systems, and combustion systems. Eliminating energy waste, often linked with increased disorder, remains a significant challenge for Scientists and Engineers. Consequently, studying entropy generation offers valuable insights for enhancing flow and heat transfer systems. Research by Reddy, Kumar, and Bég [3] on viscosity variations in viscoelastic flows, Goyal and Srinivas [4] on converting wasted energy into usable forms, and Aiyesimi *et al.* [5] on the effects of chemical reactions, magnetic fields, and Hall effects in magnetohydrodynamic flows demonstrates that a deeper understanding of entropy can improve heat transfer efficiency, reduce energy consumption, and minimize environmental impact. Additionally, entropy analysis aids in predicting fluid behaviour and refining modeling accuracy. Further exploration can be found in [6]-[10].

Unsteady reactive viscous flow in porous cylindrical pipes is critical for various engineering applications, necessitating a thorough understanding of fluid dynamics and heat transfer [11]. In chemical reactors, porous cylindrical pipes enhance the interaction between reactants and catalysts, thereby improving system performance [12]. Farayola [12] showed that adjusting thermal conductivity and viscous heating parameters in a porous cylindrical pipe with a reactive variable viscous fluid can effectively manage fluid temperature and boost system efficiency. The unsteady flow conditions and reactive processes within these reactors are crucial for optimizing reaction rates and product yields. Paul [13] explored the impact of a magnetic field on the unsteady natural convective one-dimensional laminar flow of an incompressible, slightly electrically conducting fluid over a vertical cylinder, finding that increased porosity enhances fluid velocity. Additionally, viscous dissipation is a major contributor to entropy generation by converting mechanical energy into thermal energy, which increases system disorder and affects entropy management in chemical processes [12] [14]. Shehata *et al.* [15] numerically analyzed entropy generation due to viscous dissipation around a well's turbine blade and concluded that understanding viscous dissipation enables Engineers to optimize energy inputs, improve reaction efficiency, and develop more sustainable chemical processes.

Porous cylindrical pipes are also vital in filtration systems due to their ability to facilitate unsteady flow through the porous medium, which improves particle and contaminant separation. The effectiveness of these pipes depends on factors such

as fluid dynamics, viscosity, and interactions within the filter material. Understanding entropy generation is crucial for designing filtration systems that maximize separation performance while minimizing energy costs. In thermal management applications, these pipes play a significant role in heat dissipation, essential for the safe operation of electronic devices and automotive engines [16]. Studying unsteady reactive viscous flow in these pipes allows engineers to enhance thermal conductivity and heat dissipation efficiency, resulting in better cooling performance and reduced thermal resistance [17]. The study of entropy in porous cylindrical pipes addresses several key aspects and challenges [18]. The porous structure and cylindrical geometry significantly impact fluid flow and heat transfer. While the porous medium enhances heat and mass transfer by increasing the interaction surface area, it also introduces frictional resistance and flow maldistribution, leading to additional entropy generation [19]. Accurate modeling requires considering the complex interactions between fluid dynamics, thermal effects, and reactive processes. Although isothermal wall conditions simplify thermal analysis, they may not always reflect real-world variations [20]. Additionally, experimental measurement of entropy generation and validation of theoretical models pose challenges due to the need for precise instrumentation and data interpretation. Addressing these aspects is essential for optimizing the design and performance of systems involving porous cylindrical pipes, such as heat exchangers and chemical reactors.

Despite the critical importance of analyzing entropy production for designing heat exchangers that minimize energy losses and enhance thermal performance which is key for applications requiring precise temperature control and high thermal efficiency in power plants and industrial heating systems, limited research specifically addresses entropy generation in unsteady reactive viscous flow within a porous cylindrical pipe with an isothermal wall. The objective of this paper, therefore, is to study the unsteady flow of a reactive variable viscous fluid in a porous cylindrical pipe with an isothermal wall under Arrhenius kinetics and to report the effects of porosity and heating parameters, and Prandtl number on the entropy generation of the flow.

## 2. Mathematical Formulation of the Problem

Unsteady flow of a laminar, incompressible, viscous heat generation/absorption fluid in a porous cylindrical pipe in the presence of a pressure gradient has been considered. The temperature of the wall of the cylindrical pipe is assumed to be constant throughout the flow. The radius of the pipe is $a$ unit. The governing equations of the problem with the corresponding initial and boundary conditions are stated as follows:

**Energy equation:**

$$\rho C_p\left(\frac{\partial T}{\partial \bar{t}}+\bar{V}\frac{\partial T}{\partial \bar{r}}\right)=\frac{k}{\bar{r}}\frac{\partial}{\partial \bar{r}}\left(\bar{r}\frac{\partial T}{\partial \bar{r}}\right)+QC_0A\mathrm{e}^{-\frac{E}{RT}}+\mu\left(\frac{\partial \bar{u}}{\partial \bar{r}}\right)^2 \tag{1}$$

**Momentum equation:**

$$\rho\left(\frac{\partial \bar{u}}{\partial \bar{t}}+\bar{V}\frac{\partial \bar{u}}{\partial \bar{r}}\right)=\frac{1}{\bar{r}}\frac{\partial}{\partial \bar{r}}\left(\mu \bar{r}\frac{\partial \bar{u}}{\partial \bar{r}}\right)+\frac{\mu}{k_1}\bar{u}+G \tag{2}$$

**Initial and boundary conditions:**

$$\begin{aligned}&\bar{u}\left(\bar{r},t\right)=0, \qquad T\left(\bar{r},t\right)=T_0 \quad \text{on} \quad \bar{r}=a;\\ &\bar{u}\left(\bar{r},0\right)=0, \qquad T\left(\bar{r},0\right)=0\\ &\frac{\partial T\left(\bar{r},t\right)}{\partial \bar{r}}=\frac{\partial \bar{u}\left(\bar{r},t\right)}{\partial \bar{r}}=0 \quad \text{on} \quad \bar{r}=0\end{aligned} \tag{3}$$

where $\bar{V}$ is the suction velocity, and $\rho, C_P, k, k_1, \mu, Q, C_0, A, T, \bar{u}, G$ are as defined in the nomenclature. The source term $Q$, represents the heat generation when $Q>0$ and represents the heat absorption term when $Q<0$.

Figure 1 shows the schematic diagram of problem. The flow is in the z-direction and the velocity varies along $\bar{r}$, *i.e.* velocity varies from the centre to the wall of the cylindrical pipe. There is constant concentration of the chemical species, that is, the materials are not consumed, the fluid is reactive and incompressible, and it is an Initial Boundary Value forced convention problem.

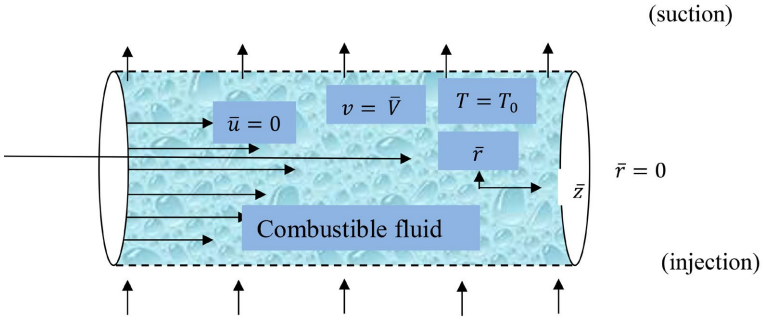


**Figure 1.** Schematic diagram of unsteady flow in a porous cylindrical pipe.

Introducing the dimensionless variables in Equation (4) into Equations (1)-(3),

$$\begin{aligned}&\theta=\frac{E}{RT_0^2}\left(T-T_0\right) \Rightarrow T=T_0+\frac{RT_0^2}{E}\theta \text{ and } \partial T=\frac{RT_0^2}{E}\partial\theta\\ &\varepsilon=\frac{RT_0^2}{E}, \quad \bar{u}=u_0u \Rightarrow \partial\bar{u}=u_0\partial u, \bar{n}=\frac{V_0^2 n}{\nu}\\ &\bar{t}=\frac{\nu t}{V_0^2} \Rightarrow \frac{\partial}{\partial \bar{t}}=\frac{1}{\nu/V_0^2}\frac{\partial}{\partial t} \text{ and } \frac{\partial}{\partial \bar{t}}=\frac{V_0^2}{\nu}\frac{\partial}{\partial t}\\ &\bar{r}=\frac{\nu r}{V_0} \Rightarrow \partial\bar{r}=\frac{\nu}{V_0}\partial r \text{ and } \frac{\partial}{\partial \bar{r}}=\frac{V_0}{\nu}\frac{\partial}{\partial r}\end{aligned} \tag{4}$$

we have

$$\frac{\partial\theta}{\partial t}-\left(1+\varepsilon A_* e^{nt}\right)\frac{\partial\theta}{\partial r}=\frac{1}{Pr}\frac{1}{r}\frac{\partial}{\partial r}\left(r\frac{\partial\theta}{\partial r}\right)+\frac{\lambda}{Pr}e^{\frac{\theta}{1+\varepsilon\theta}}+\lambda He\cdot e^{\frac{-\theta}{1+\varepsilon\theta}}\left(\frac{\partial u}{\partial r}\right)^2 \tag{5}$$

$$\frac{\partial u}{\partial t}-\left(1+\varepsilon A_* e^{nt}\right)\frac{\partial u}{\partial r}=\frac{\delta}{r}\frac{\partial}{\partial r}\left(e^{\frac{-\theta}{1+\varepsilon\theta}}r\frac{\partial u}{\partial r}\right)+\delta_1 e^{\frac{-\theta}{1+\varepsilon\theta}}u+1 \tag{6}$$

with dimensionless initial and boundary conditions

$$\begin{aligned} &\theta(1,t)=u(1,t)=0, && \theta(r,0)=\theta_c(r) \\ &u(r,0)=h(r), && \frac{\partial\theta}{\partial r}(0,t)=\frac{\partial u}{\partial r}(0,t)=0 \end{aligned} \tag{7}$$

where

$\lambda=\dfrac{QEAa^2C_0\mathrm{e}^{-\frac{E}{RT_0}}}{kRT_0^2}=\dfrac{QEAv^2C_0\mathrm{e}^{-\frac{E}{RT_0}}}{kRT_0^2V_0^2}$ (the Frank-Kamenetskii parameter), $He=\dfrac{k\mu_0u_0^2V_0^2\mathrm{e}^{\frac{2E}{RT_0}}}{\rho C_Pv^3QAC_0}$ (the viscous heating parameter), $a^2=\dfrac{v^2}{V_0^2}$, $P_r=\dfrac{\rho C_pv}{k}$ (the Prandtl number), $\delta=\dfrac{V_0}{v}\mathrm{e}^{\frac{E}{RT_0}}>0$, $V_0\ll1$ (the suction parameter), $G=\dfrac{\rho u_0V_0^2}{v}$ (the constant axial pressure gradient), and $\delta_1=\dfrac{v\mu_0\mathrm{e}^{\frac{E}{RT_0}}}{\rho V_0^2k_1}=\dfrac{v^2\mathrm{e}^{\frac{E}{RT_0}}}{V_0^2k_1}$ (the porosity (permeability) parameter).

The suction velocity takes the exponential form

$$\bar{V}=-V_0\left(1+\varepsilon A_*\mathrm{e}^{\overline{nt}}\right) \tag{8}$$

where $A_*$ is a real positive constant, $\varepsilon$ and $\varepsilon A_*$ are small less than unity, and $V_0$ is a scale suction velocity which has non-zero positive constant [21]-[24], and in non-dimensional form, $\bar{V}$ can be written as

$$\bar{V}=-V_0\left(1+\varepsilon A_*\mathrm{e}^{nt}\right) \tag{9}$$

For all fuels of interest, the parameter $\varepsilon$ is assumed to be small. By using the method of activation energy asymptotics and for $\varepsilon\ll1$, it gives [25]-[27]

$$\frac{\partial\theta}{\partial t}-\left(1+\varepsilon A_*\mathrm{e}^{nt}\right)\frac{\partial\theta}{\partial r}=\frac{1}{Pr}\frac{1}{r}\frac{\partial}{\partial r}\left(r\frac{\partial\theta}{\partial r}\right)+\lambda\left(\frac{1}{Pr}\mathrm{e}^{\theta}+He\cdot\mathrm{e}^{-\theta}\left(\frac{\partial u}{\partial r}\right)^2\right). \tag{10}$$

and

$$\frac{\partial u}{\partial t}-\left(1+\varepsilon A_*\mathrm{e}^{nt}\right)\frac{\partial u}{\partial r}=\frac{\delta}{r}\frac{\partial}{\partial r}\left(\mathrm{e}^{-\theta}r\frac{\partial u}{\partial r}\right)+\delta_1\mathrm{e}^{-\theta}u+1 \tag{11}$$

with the dimensionless initial and boundary conditions

$$\begin{aligned} &\theta(1,t)=u(1,t)=0, && \theta(r,0)=\theta_c(r) \\ &u(r,0)=h(r), && \frac{\partial\theta}{\partial r}(0,t)=\frac{\partial u}{\partial r}(0,t)=0 \end{aligned} \tag{12}$$

The coupled nonlinear partial differential equations with the initial and boundary conditions are difficult to solve to obtain exact solutions. And since the cylindrical coordinate has singularity at $r=0$, singular perturbation technique was employed as it was obtained in [8] [28] and the solutions are assumed to be of the form:

$$u(r,t)=u_0(r)+\varepsilon\mathrm{e}^{nt}u_1(r)+0\left(\varepsilon^2\right) \tag{13}$$

$$\theta(r,t)=\theta_0(r)+\varepsilon e^{nt}\theta_1(r)+0(\varepsilon^2) \tag{14}$$

Now,

$$e^{\theta(r,t)}=e^{\theta_0(r)}\left(1+\varepsilon e^{nt}\theta_1(r)\right) \quad \text{neglecting} \quad 0(\varepsilon^2) \tag{15}$$

and

$$e^{-\theta(r,t)}=e^{-\theta_0(r)}\left(1-\varepsilon e^{nt}\theta_1(r)\right) \quad \text{neglecting} \quad 0(\varepsilon^2) \tag{16}$$

Substituting Equations (13), (14), (15) and (16) in Equations (10) and (11), and setting $\lambda=\varepsilon e^{nt}\Lambda$, in Equation (10) gives

$$\begin{aligned} &n\varepsilon e^{nt}\theta_1(r)-\left(1+\varepsilon A_* e^{nt}\right)\frac{\partial}{\partial r}\left[\theta_0(r)+\varepsilon e^{nt}\theta_1(r)\right] \\ &=\frac{1}{Pr}\frac{1}{r}\frac{\partial}{\partial r}\left(r\frac{\partial}{\partial r}\left(\theta_0(r)+\varepsilon e^{nt}\theta_1(r)\right)\right)+\varepsilon e^{nt}\Lambda\left[\frac{1}{Pr}e^{\theta_0(r)}\left(1+\varepsilon e^{nt}\theta_1(r)\right)\right. \\ &\left.+He\cdot e^{-\theta_0(r)}\left(1-\varepsilon e^{nt}\theta_1(r)\right)\left[\frac{\partial}{\partial r}\left(u_0(r)+\varepsilon e^{nt}u_1(r)\right)\right]^2\right] \end{aligned} \tag{17}$$

and

$$\begin{aligned} &n\varepsilon e^{nt}u_1(r)-\left(1+\varepsilon A_* e^{nt}\right)\frac{\partial}{\partial r}\left(u_0(r)+\varepsilon e^{nt}u_1(r)\right) \\ &=\frac{\delta}{r}\frac{\partial}{\partial r}\left[e^{-\theta_0(r)}\left(1-\varepsilon e^{nt}\theta_1(r)\right)\frac{\partial}{\partial r}\left(u_0(r)+\varepsilon e^{nt}u_1(r)\right)\right] \\ &+\delta_1 e^{-\theta_0(r)}\left(1-\varepsilon e^{nt}\theta_1(r)\right)\left(u_0(r)+\varepsilon e^{nt}u_1(r)\right)+1 \end{aligned} \tag{18}$$

Equating powers of $\varepsilon$ and simplifying Equations (17) & (18), and applying the dimensionless initial and boundary conditions in Equation (12), we have

$$\theta(r,t)=\varepsilon e^{nt}\left(a_4+a_{10}r^2+a_9r^3+a_8r^4+a_7r^5+a_6r^6+a_5r^7\right) \tag{19}$$

$$u(r,t)=a_1+a_2r^3+a_3r^5+\varepsilon e^{nt}\left(a_{11}+a_{12}r^3+a_{13}r^5\right) \tag{20}$$

where

$$a_1=\frac{20\delta-3}{120\delta^2-20\delta\delta_1+3\delta_1} \tag{21}$$

$$a_2=-\frac{1}{6\delta}\left[1+\frac{\delta_1(20\delta-3)}{120\delta^2-20\delta\delta_1+3\delta_1}\right] \tag{22}$$

$$a_3=\frac{1}{40\delta^2}\left[1+\frac{\delta_1(20\delta-3)}{120\delta^2-20\delta\delta_1+3\delta_1}\right] \tag{23}$$

$$\begin{aligned} a_4=&\frac{\Lambda\left(-6350400+1411200Pr-264600Pr^2-396900nPr+42336Pr^3\right.}{-25401600-6350400nPr+1411200nPr^2-264600nPr^3-396900n^2Pr} \\ &\left.-5880Pr^4+3804nPr^4+3798n^2Pr^3+777600Hea_2^2Pr^2+270Pr^5\right) \\ &+42336nPr^4+119952n^2Pr^3-5880nPr^5-24010n^2Pr^4-11025n^3Pr^3 \\ &+720nPr^6+3798n^3Pr^4+3804n^2Pr^5 \end{aligned} \tag{24}$$

$$\begin{aligned} a_5 = &-\frac{1}{4233600}a_4\left(120nPr^2+633n^3+634n^2Pr\right)Pr^4 \\ &+\frac{1}{1225}\left(-\frac{1}{4}\left(-\frac{1}{6}\Lambda Pr^2-\frac{1}{4}\Lambda nPr\right)Pr+\frac{1}{18}\Lambda Pr^2n\right)nPr \\ &-\frac{1}{294}\left(-9\Lambda He\cdot a_2^2Pr+\frac{1}{16}\left(-\frac{1}{6}\Lambda Pr^2-\frac{1}{4}\Lambda nPr\right)nPr\right. \\ &\left.-\frac{1}{5}\left(-\frac{1}{4}\left(-\frac{1}{16}\Lambda Pr^2-\frac{1}{4}\Lambda nPr\right)Pr+\frac{1}{18}\Lambda Pr^2n\right)Pr\right)Pr \end{aligned} \tag{25}$$

$$\begin{aligned} a_6 = &\frac{a_4}{103680}\left(24nPr^2+98n^2Pr+45n^3\right)Pr^3 \\ &-\frac{1}{4}\Lambda He\cdot a_2^2Pr+\frac{1}{576}\left(-\frac{1}{6}\Lambda Pr^2-\frac{1}{4}\Lambda nPr\right)nPr \\ &-\frac{1}{180}\left(-\frac{1}{4}\left(-\frac{1}{6}\Lambda r^2-\frac{1}{4}\Lambda nPr\right)Pr+\frac{1}{18}\Lambda Pr^2n\right)Pr \end{aligned} \tag{26}$$

$$a_7 = -\frac{1}{100}\left(-\frac{1}{6}\Lambda Pr^2-\frac{1}{4}\Lambda nPr\right)Pr+\frac{1}{450}\Lambda Pr^2n-\frac{1}{3600}a_4\left(6nPr+17n^2\right)Pr^3 \tag{27}$$

$$a_8 = -\frac{1}{96}\Lambda Pr^2-\frac{1}{64}\Lambda nPr+\frac{1}{192}a_4\left(2nPr+3n^2\right)Pr^2 \tag{28}$$

$$a_9 = -\frac{1}{18}a_4nPr^2+\frac{1}{18}\Lambda Pr \tag{29}$$

$$a_{10} = -\frac{1}{4}a_4nPr+\frac{1}{4}\Lambda \tag{30}$$

$$\begin{aligned} a_{11} = &-\frac{1}{120\delta^2+20\delta n-20\delta_1\delta-3n+3\delta_1}\left(-18Aa_2\delta+6\delta_1a_{10}a_1\delta+20\delta\delta_1a_4a_1\right. \\ &\left.+120\delta^2a_4a_2+120\delta^2a_4a_3+72\delta^2a_{10}a_2-3\delta_1a_4a_1-18\delta a_4a_2\right) \end{aligned} \tag{31}$$

$$a_{12} = \frac{1}{6\delta}\left(na_{11}+\delta_1a_4a_1+6\delta a_4a_2-\delta_1a_{11}\right) \tag{32}$$

$$\begin{aligned} a_{13} = &-\frac{1}{40\delta^2}\left(-2\delta_1a_{10}a_1\delta-40\delta^2a_4a_3-24\delta^2a_{10}a_2+6Aa_2\delta\right. \\ &\left.+na_{11}+\delta_1a_4a_1+6\delta a_4a_2-\delta_1a_{11}\right) \end{aligned} \tag{33}$$

## 3. Dimensionless Entropy Generation Rate

Okedoye, Lamidi and Ayeni [29] defined the two-dimensionless entropy generation rate as:

$$\Gamma_n = \left(\frac{\partial\theta}{\partial y}\right)^2+\lambda_1\left(\frac{\partial u}{\partial y}\right)^2+\lambda_2\left(\frac{\partial c}{\partial y}\right)^2+\lambda_3\left(\frac{\partial\theta}{\partial y}\right)\left(\frac{\partial c}{\partial y}\right) \tag{34}$$

The following can now be defined:

$$\Gamma_{n,h} = \left(\frac{\partial\theta}{\partial y}\right)^2,\ \Gamma_{n,f} = \lambda_1\left(\frac{\partial u}{\partial y}\right)^2,\ \Gamma_{n,d}^{c} = \lambda_2\left(\frac{\partial c}{\partial y}\right)^2,\ \text{and}\ \Gamma_{n,d}^{c,T} = \lambda_3\left(\frac{\partial\theta}{\partial y}\right)\left(\frac{\partial c}{\partial y}\right),$$

where $\Gamma_{n,h}$ and $\Gamma_{n,f}$ are thermal and viscous irreversibility respectively, while $\Gamma_{n,d}^{c}+\Gamma_{n,d}^{c,T}$ is the diffusive irreversibility. Dimensionless terms denoted by

$\lambda_i \left(1 \le i \le 3\right)$, and called irreversibility distribution ratios, are given by:

$$\lambda_1 = \frac{\mu T_0}{k}\left(\frac{a}{L(\Delta T)}\right)^2, \quad \lambda_2 = \frac{RDT_0}{kc_0}\left(\frac{\Delta c}{\Delta T}\right)^2, \quad \lambda_3 = \frac{RD}{k}\left(\frac{\Delta c}{\Delta T}\right)$$

where $C_0$ and $T_0$ are respectively the reference concentration and temperature, which are in our case, the bulk concentration and the bulk temperature.

Now for the discussion, obtained solutions in Equations (19) and (20) are made use of, which are respectively

$$\theta(r,t) = \varepsilon \mathrm{e}^{nt}\left(a_4 + a_{10}r^2 + a_9 r^3 + a_8 r^4 + a_7 r^5 + a_6 r^6 + a_5 r^7\right)$$

$$u(r,t) = a_1 + a_2 r^3 + a_3 r^5 + \varepsilon \mathrm{e}^{nt}\left(a_{11} + a_{12}r^3 + a_{13}r^5\right)$$

representing both energy and velocity distributions. Since the model does not involve chemical species, we have that $\lambda_3 = 0$. Therefore Equation (34) becomes

$$\Gamma_n = \left(\frac{\partial \theta}{\partial r}\right)^2 + \lambda_1\left(\frac{\partial u}{\partial r}\right)^2$$

*i.e.*

$$\begin{aligned}\Gamma_n = &\left(3a_2 r^2 + 5a_3 r^4 + \varepsilon \mathrm{e}^{nt}\left(3a_{12}r^2 + 5a_{13}r^4\right)\right)^2 \\ &+ \lambda_1\left(\varepsilon \mathrm{e}^{nt}\left(2a_{10}r + 3a_9 r^2 + 4a_8 r^3 + 5a_7 r^4 + 6a_6 r^5 + 7a_5 r^7\right)\right)^2\end{aligned} \tag{35}$$

where

$a_1$, $a_2$, $a_3$, $a_4$, $a_5$, $a_6$, $a_7$, $a_8$, $a_9$, $a_{10}$, $a_{11}$, $a_{12}$, $a_{13}$ are as defined in Equations (21), (22), (23), (24), (25), (26), (27), (28), (29), (30), (31), (32), (33) respectively.

## 4. Results and Discussion

The graph of Entropy generation rate against $r$ for various flow parameters are shown in Figure 2 and Figure 3. Figure 2 shows the permeability parameter ($\delta_1$) with the entropy generation rate. Entropy against $r$ with different values of Prandtl number (*Pr*) are shown in Figure 3 while the graph of entropy generation rate with different values of viscous heating parameter (*He*) are displayed in Figure 4. Figure 5 shows the 3D graph of Entropy against $r$ and permeability parameter.

In Figure 2, the entropy generation rate against $r$ for various values of permeability parameter is displayed. It is observed that the degree of disorderliness in the fluid is high towards the wall of the cylindrical pipe and maximum entropy is observed to be between $r = 0.8$ and $r = 0.9$ away from the centre of the cylindrical pipe. As permeability parameter increases, the degree of disorderliness increases until when permeability parameter approaches 4.2887, a point at which entropy run away *i.e.* blow up. This is depicted in Figure 5 where the value of the entropy generation rate approaches infinity.

Figure 3 shows the graph of entropy generation rate against $r$ for different

values of Prandtl number. It is observed that increase in Prandtl number causes increase in entropy with the effect felt halfway towards the wall of the cylindrical pipe. This is in line with the results of [7] [9] [14], where it was observed that increasing the Prandtl number decreases the entropy generation firstly around the pipe centreline, then it enhances entropy rapidly towards the pipe wall, which supports the findings of [18] [21] [22]. The combined effect of Prandtl number on velocity and entropy generation rate is that as the Prandtl number increases, the velocity decreases towards the wall of the cylindrical pipe while the entropy generation rate increases towards the wall of the pipe.

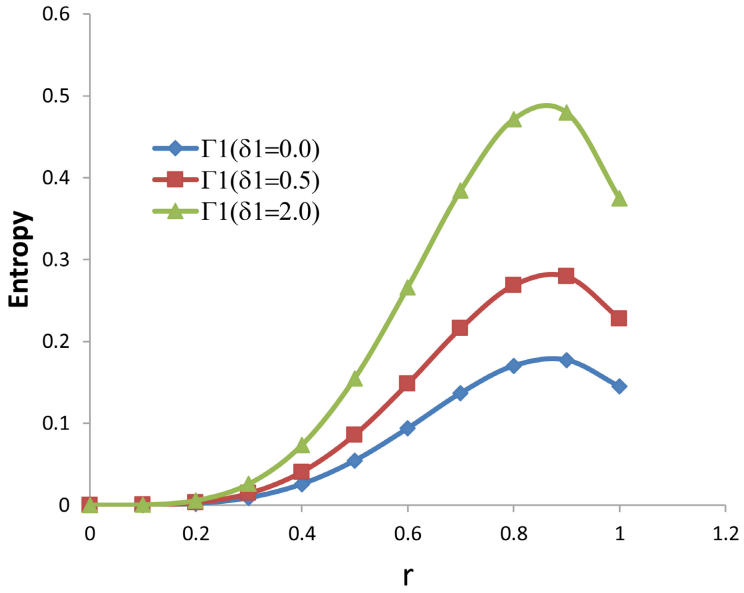


**Figure 2.** Profile of Entropy against $r$ for different values of Permeability parameter ($\delta_1$) when $Pr = 0.71$, $He = 1.0$, $\epsilon = 0.01$, $n = 0.1$, $\Lambda = 45.24$, $\delta = 1.25$, $\beta = 0.5$, $t = 1.0$.

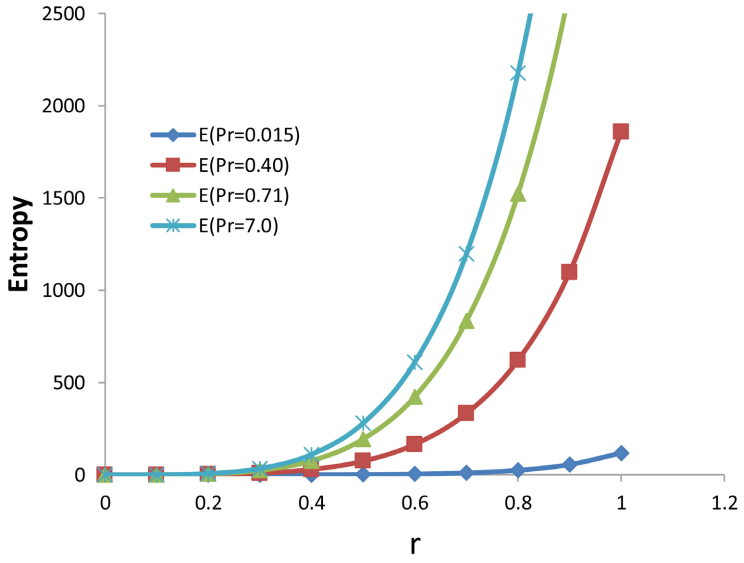


**Figure 3.** Plots of Entropy against $r$ for different values of Prandtl number ($Pr$) when $He = 1.0$, $\delta_1 = 1.0$, $\epsilon = 0.01$, $n = 0.1$, $\Lambda = 45.24$, $\delta = 1.25$, $\beta = 0.5$, $t = 1.0$.

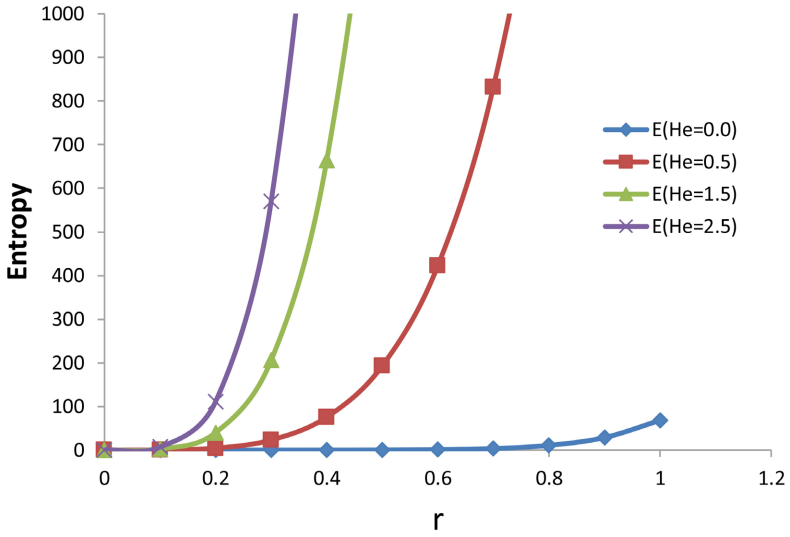


**Figure 4.** Plots of Entropy against $r$ for different values of Heating parameter ($He$) when $Pr = 1.0$, $\delta_1 = 1.0$, $\epsilon = 0.01$, $n = 0.1$, $\Lambda = 45.24$, $\delta = 1.25$, $\beta = 0.5$, $t = 1.0$.

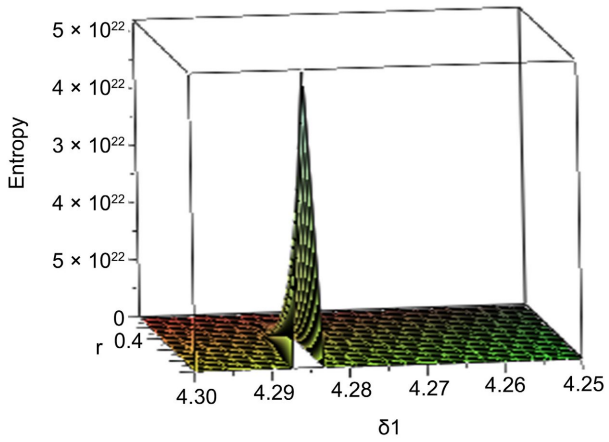


**Figure 5.** Plots of Entropy against $r$ and $\delta_1$ when $He = 0.5$, $Pr = 1.0$, $\epsilon = 0.01$, $n = 0.1$, $\Lambda = 45.24$, $\delta = 1.25$, $\beta = 0.5$, $t = 1.0$.

Similar trend is observed in **Figure 4** where increase in viscous heating parameter causes increase in entropy generation [26] [28]. This is obvious as increase in heat energy usually agitates the molecules of the fluid and hence increase the rate of disorderliness in the fluid.

## 5. Conclusions

This study provided an in-depth analysis of entropy generation in an unsteady reactive viscous flow within a porous cylindrical pipe with an isothermal wall. By investigating key flow parameters namely: permeability, viscous heating, and the Prandtl number, the following key findings were established regarding the behaviour of entropy within the system:

1) Entropy distribution in the flow field: The degree of disorderliness within the fluid was found to be significantly high near the wall of the cylindrical pipe. This

is attributed to the interaction between thermal and viscous forces, which leads to enhanced irreversible energy dissipation in the boundary layer region.

2) Radial Entropy Peak: The analysis revealed that maximum entropy generation occurs within the radial range r = 0.8 to r = 0.9, away from the centre of the pipe. This suggests that entropy generation is not uniformly distributed but is concentrated in regions where thermal gradients and fluid velocity interactions are pronounced.

3) Effect of Permeability: Increasing the permeability parameter generally leads to a rise in entropy generation, indicating intensified fluid interaction within the porous medium. However, when the permeability parameter reaches **4.2887**, the system undergoes a critical transition, causing entropy generation to diverge. This suggests that beyond this threshold, the porous structure significantly alters the flow dynamics, potentially introducing instability.

4) Influence of Prandtl Number on the entropy: A higher Prandtl number corresponds to increased entropy generation, with the effect becoming more pronounced midway toward the pipe's wall. Since the Prandtl number governs the ratio of momentum diffusivity to thermal diffusivity, its influence on entropy highlights the strong interplay between heat conduction and viscous dissipation within the system.

Overall, the study offers important insights into the thermodynamic behavior of porous pipe flows, with implications for the design and optimization of thermal systems such as heat exchangers and energy-efficient industrial processes.

## 6. Applications

Entropy generation is a crucial concept in assessing the efficiency and performance of diverse engineering systems, particularly those involving fluid flow, heat transfer, and reactive processes, where optimizing energy utilization and minimizing losses are paramount. The findings of the study provide actionable insights for several applications, with quantifiable benefits in efficiency, energy savings, and system reliability.

The findings on entropy generation can guide the design of heat exchangers with improved thermal efficiency. And by optimizing permeability and viscous heating parameters, engineers can achieve between 5% and 15% reduction in thermal losses, resulting in improved heat transfer efficiency [7] [16] [30]. The entropy trends observed in this study can help determine the ideal material selection and flow control strategies to minimize energy dissipation in heat exchangers. Chemical reactors rely on efficient mixing and heat transfer to maximize reaction rates while minimizing energy losses. Adjusting permeability parameters based on entropy generation analysis can enhance mixing efficiency, potentially increasing reaction yield between 10% and 20% in industrial chemical processes [30]. The study's insights can be used to design reactors with optimized flow conditions, reducing entropy-related inefficiencies in large-scale production.

In porous media, structures are used in filtration systems, petroleum extraction,

and biomedical fluid transport. Engineers can use entropy-based optimization to design porous structures that increase fluid transport efficiency between 8% and 12% while minimizing entropy-dependent losses [31]. The findings can inform the development of advanced filtration membranes and enhanced oil recovery techniques. Entropy generation directly affects energy consumption in industrial systems, including turbines, compressors, and fluid transport networks. By implementing entropy-based design modifications, industries can achieve between 3% and 7% reductions in overall energy consumption, leading to significant cost savings [32]. The study's results can be integrated into computational models for predictive maintenance and system optimization.

## Acknowledgements

I appreciate the Tertiary Education Trust Fund (TETFund), Abuja, Nigeria for sponsoring me, on behalf of other authors of this paper, to attend the 2025 Joint Mathematics Meeting (2025 JMM) organized by the American Mathematical Society held at Seattle, WA, USA between 8 and 11 January 2025, and the Management of Emmanuel Alayande University of Education, Oyo, Nigeria for releasing me to attend this 2025 JMM for the first time.

## Conflicts of Interest

The authors declare no conflicts of interest regarding the publication of this paper.

## References

[1] Wang, Z. (2022) The Entropy Perspective on Human Illness and Aging. *Engineering*, **9**, 22-26. https://doi.org/10.1016/j.eng.2021.08.014

[2] Sauerheber, R. (2018) Thermodynamics and Entropy in Natural and Artificial Systems. *American Research Journal of Chemistry*, **2**, 1-26.

[3] Janardhana Reddy, G., Kumar, M. and Anwar Beg, O. (2018) Effect of Temperature Dependent Viscosity on Entropy Generation in Transient Viscoelastic Polymeric Fluid Flow from an Isothermal Vertical Plate. *Physica A*: *Statistical Mechanics and Its Applications*, **510**, 426-445. https://doi.org/10.1016/j.physa.2018.06.065

[4] Goyal, K. and Srinivas, S. (2023) Entropy Generation Analysis for Hydromagnetic Two-Layered Pulsatile Immiscible Flow with Joule Heating and First-Order Chemical Reaction. *Case Studies in Thermal Engineering*, **47**, Article ID: 103046. https://doi.org/10.1016/j.csite.2023.103046

[5] Aiyesimi, Y.M., Jiya, M., Bolarin, G.A. and Akinremi, O.V. (2019) Entropy Generation Analysis of a Reactive MHD Third Grade Fluid in a Cylindrical Pipe with Radially Applied Magnetic Field and Hall Current. *Asian Research Journal of Mathematics*, **12**, 1-20. https://doi.org/10.9734/arjom/2019/v12i330086

[6] Janardhana Reddy, G., Bhaskerreddy, K., Mahesh, K. and Anwar Bég, O. (2019) Transient Analysis of Casson Fluid Thermo-Convection from a Vertical Cylinder Embedded in a Porous Medium: Entropy Generation and Thermal Energy Transfer Visualization. *Journal of Central South University*, **26**, 1342-1361. https://doi.org/10.1007/s11771-019-4091-x

[7] Raje, A., Koyani, F., Bhise, A.A. and Ramesh, K. (2023) Heat Transfer and Entropy Optimization for Unsteady MHD Casson Fluid Flow through a Porous Cylinder: Ap-

plications in Nuclear Reactors. *International Journal of Modern Physics B*, **37**, 1-21. https://doi.org/10.1142/s0217979223502934

[8] Khan, M., Shahid, A., El Shafey, M., Salahuddin, T. and Khan, F. (2020) Predicting Entropy Generation in Flow of Non-Newtonian Flow Due to a Stretching Sheet with Chemically Reactive Species. *Computer Methods and Programs in Biomedicine*, **187**, Article ID: 105246. https://doi.org/10.1016/j.cmpb.2019.105246

[9] Panya, A.L., Akinyemi, O.A. and Okedoye, A.M. (2023) Entropy Generation in Unsteady MHD Convective Flow Past a Flat Porous Oscillating Plate with Suction or Injection. *Global Journal of Engineering and Technology Advances*, **14**, 107-127. https://doi.org/10.30574/gjeta.2023.14.2.0037

[10] Sadiki, A., Agrebi, S. and Ries, F. (2022) Entropy Generation Analysis in Turbulent Reacting Flows and near Wall: A Review. *Entropy*, **24**, Article No. 1099. https://doi.org/10.3390/e24081099

[11] Sharma, K.R. and Jain, S. (2024) An Unsteady MHD Williamson Fluid Flow in a Vertical Porous Channel with Porous Media and Thermal Radiation. *International Journal of Advances in Engineering Sciences and Applied Mathematics*, **16**, 274-285. https://doi.org/10.1007/s12572-024-00371-w

[12] Farayola, P.I. (2017) On Steady Flow of a Reactive Viscous Fluid in a Porous Cylindrical Pipe. *Open Journal of Fluid Dynamics*, **7**, 359-370. https://doi.org/10.4236/ojfd.2017.73024

[13] Paul, A. (2022) Magnetohydrodynamic Unsteady Natural Convective Flow in a Porous Medium over a Moving Infinite Cylinder. *Heat Transfer*, **51**, 6548-6562. https://doi.org/10.1002/htj.22612

[14] Wei Ting, T., Mun Hung, Y. and Guo, N. (2016) Viscous Dissipation Effect on Streamwise Entropy Generation of Nanofluid Flow in Microchannel Heat Sinks. *Journal of Energy Resources Technology*, **138**, Article ID: 052002. https://doi.org/10.1115/1.4032792

[15] Shehata, A.S., Saqr, K.M., Shehadeh, M., Xiao, Q. and Day, A.H. (2014) Entropy Generation Due to Viscous Dissipation around a Wells Turbine Blade: A Preliminary Numerical Study. *Energy Procedia*, **50**, 808-816. https://doi.org/10.1016/j.egypro.2014.06.099

[16] Cheng, X. and Liang, X. (2017) Role of Entropy Generation Minimization in Thermal Optimization. *Chinese Physics B*, **26**, Article ID: 120505. https://doi.org/10.1088/1674-1056/26/12/120505

[17] Maleki, H., Safaei, M.R., Togun, H. and Dahari, M. (2018) Heat Transfer and Fluid Flow of Pseudo-Plastic Nanofluid over a Moving Permeable Plate with Viscous Dissipation and Heat Absorption/generation. *Journal of Thermal Analysis and Calorimetry*, **135**, 1643-1654. https://doi.org/10.1007/s10973-018-7559-2

[18] Ijaz, S., Mushtaq, M., Munawar, S. and Saleem, N. (2018) Entropy Generation Minimisation in a Moving Porous Pipe under Magnetic Field Effect. *International Journal of Exergy*, **26**, 418-434. https://doi.org/10.1504/ijex.2018.093187

[19] Kumaresan, G., Vijayakumar, P., Ravikumar, M., Kamatchi, R. and Selvakumar, P. (2018) Experimental Study on Effect of Wick Structures on Thermal Performance Enhancement of Cylindrical Heat Pipes. *Journal of Thermal Analysis and Calorimetry*, **136**, 389-400. https://doi.org/10.1007/s10973-018-7842-2

[20] Shockner, T., Salman, I., Van Riet, V., Beyne, W., De Paepe, M., Degroote, J., *et al.* (2024) Simultaneous Close-Contact Melting on Two Asymmetric Surfaces: Demonstration, Modeling and Application to Thermal Storage. *International Journal of Heat and Mass Transfer*, **232**, Article ID: 125950. https://doi.org/10.1016/j.ijheatmasstransfer.2024.125950

[21] Mohamed, R.A. (2009) Double-Diffusive Convection-Radiation Interaction on Unsteady MHD Flow over a Vertical Moving Porous Plate with Heat Generation and Soret Effects. *Applied Mathematical Sciences*, **3**, 629-651.

[22] Olanrewaju, P.O. and Lamidi, O.T. (2010) On the Influence of Buoyancy and Suction/Injection in Heat and Mass Transfer Problems. *Journal of the Nigerian Association of Mathematical Physics*, **16**, 293-300.

[23] Roja, P., Reddy, T.S. and Reddy, N.B. (2012) Double-Diffusive Convection-Radiation Interaction on Unsteady MHD Flow of a Micropolar Fluid over a Vertical Moving Porous Plate Embedded in a Porous Medium with Heat Generation and Soret Effects. *The International Journal of Engineering and Sciences*, **1**, 201-214.

[24] Oahimire, J.I., Olajuwon, B.I., Waheed, M.A. and Abiala, I.O. (2013) Analytical Solution to MHD Micropolar Fluid Flow past a Vertical Plate in a Slip-Flow Regime in the Presence of Thermal Diffusion and Thermal Radiation. *Journal of the Nigerian Mathematical Society*, **32**, 33-60.

[25] Bebernes, J. and Eberly, D. (1989) Mathematical Problems from Combustion Theory. Springer-Verlag, 6-8.

[26] Makinde, O.D. (2007) On Steady Flow of a Reactive Variable Viscosity Fluid in a Cylindrical Pipe with an Isothermal Wall. *International Journal of Numerical Methods for Heat & Fluid Flow*, **17**, 187-194. https://doi.org/10.1108/09615530710723957

[27] Gbadeyan, J.A. and Hassan, A.R. (2012) Multiplicity of Solutions for a Reactive Variable Viscous Couette Flow under Arrhenius Kinetics. *Mathematical Theory and Modelling*, **2**, 39-49.

[28] Biswas, S. and Pal, D. (2025) Entropy-Driven Optimization of Convective Heat Transport of a Chemically Reactive Fluid in a Porous Medium with Induced Magnetic Field. *Thermal Advances*, **2**, Article ID: 100015. https://doi.org/10.1016/j.thradv.2024.100015

[29] Okedoye, A.M., Lamidi, O.T. and Ayeni, R.O. (2007) Entropy Generation in Magnetohydrodynamic (MHD) Flow of Uniformly Stretched Vertical Permeable Surface in the Presence of Heat Generation/Absorption and Chemical Reaction. *abacus*. *The Journal of Mathematical Association of Nigeria* (*MAN*), **34**, 52-57.

[30] Nabwey, H.A., Ashraf, M., Nadeem, H., Rashad, A.M. and Chamkha, A.J. (2024) Optimizing Renewable Energy Systems: A Comprehensive Review of Entropy Generation Minimization. *AIP Advances*, **14**, Article ID: 120702. https://doi.org/10.1063/5.0245560

[31] Yang, Y., Bruns, S., Stipp, S.L.S. and Sørensen, H.O. (2018) Patterns of Entropy Production in Dissolving Natural Porous Media with Flowing Fluid. *PLOS ONE*, **13**, e0204165. https://doi.org/10.1371/journal.pone.0204165

[32] Abdelhameed, T.N. (2024) Entropy Generation Analysis for Magnetohydrodynamic Flow of Chemically Reactive Fluid Due to an Accelerated Plate. *Beni-Suef University Journal of Basic and Applied Sciences*, **13**, Article No. 37. https://doi.org/10.1186/s43088-024-00497-7

## Nomenclature

| | |
|---|---|
| $\lambda$ | is the Frank-Kamenetskii parameter |
| $\rho$ | is the density of the fluid |
| $C_P$ | is the Specific Heat capacity of the fluid |
| $He$ | is the viscous heating parameter |
| $\varepsilon$ | is the activation energy parameter |
| $\mu$ | is the dynamic viscosity |
| $\mu_0$ | is the fluid reference viscosity |
| $\delta$ | is the suction parameter |
| $\theta$ | is the dimensionless temperature |
| $u$ | is the dimensionless velocity |
| $T$ | is the absolute temperature |
| $G$ | is the constant axial pressure gradient |
| $T_0$ | is the wall reference temperature |
| $k$ | is the thermal conductivity of the material |
| $E$ | is the activation energy |
| $R$ | is the universal gas constant |
| $a$ | is the pipe characteristic radius |
| $Q$ | is the heat of reaction |
| $C_0$ | is the initial concentration of the reactant species |
| $A$ | is the Arrhenius constant |
| $\overline{u}$ | is the fluid axial velocity |
| $(\overline{z},\overline{r})$ | is the distance measured in the axial and radial directions respectively. |
| $k_1$ | is the Darcy Permeability constant |
| $\delta_1$ | is the permeability parameter for the unsteady flow |